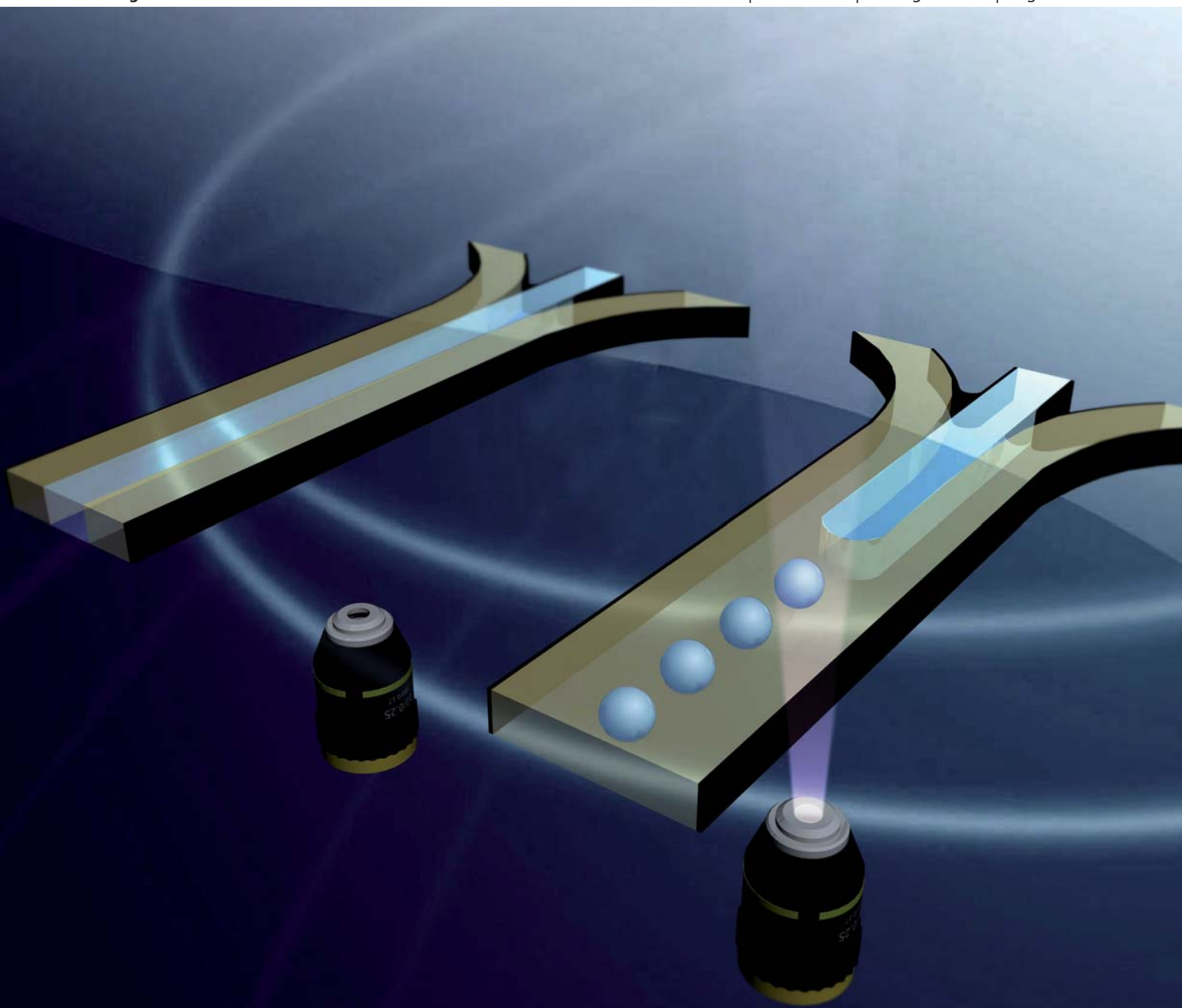


# Lab on a Chip

Miniaturisation for chemistry, physics, biology and bioengineering

[www.rsc.org/loc](http://www.rsc.org/loc)

Volume 11 | Number 16 | 21 August 2011 | Pages 2639–2796



ISSN 1473-0197

RSC Publishing

**COMMUNICATION**

Baigl *et al.*

Photoreversible fragmentation of a liquid interface for micro-droplet generation by light actuation



1473-0197 (2011) 11:16;1-0

Cite this: *Lab Chip*, 2011, **11**, 2666

www.rsc.org/loc

## Photoreversible fragmentation of a liquid interface for micro-droplet generation by light actuation†

Antoine Diguët,<sup>abc</sup> Hao Li,<sup>d</sup> Nicolas Queyriaux,<sup>abc</sup> Yong Chen<sup>abcd</sup> and Damien Baigl<sup>\*abc</sup>

Received 19th April 2011, Accepted 16th June 2011

DOI: 10.1039/c1lc20328b

We describe a method to induce by light a reversible switch from a continuous two-phase laminar flow to a droplet generating regime, in microfluidic devices with a usual water-in-oil flow focusing geometry. It consists in adding a photosensitive surfactant to the aqueous phase to modulate using light the interfacial energy between flowing liquids and the microfluidic substrate. We show that UV irradiation induces liquid fragmentation into monodisperse water microdroplets and that many cycles of reversible and rapid switches (<2 s) between continuous laminar flows and stable droplet regimes can be realized. By spatially controlling the application of the light stimulus, we also demonstrate the first spatially resolved remote induction of droplet generation.

Over the last decade, droplet-based microfluidics has been shown as a promising technology for research in biology and chemistry.<sup>1</sup> To generate micro-scale droplets, it is necessary to increase and fragment the interface between two immiscible liquids, which is usually achieved by mechanical actuation and hydrodynamic shear forces.<sup>2</sup> High-throughput emulsification with a narrow size polydispersity is usually obtained with appropriate channel junction geometry, which can be a T-junction or a flow focusing device.<sup>3</sup> For given geometry and fluid composition, droplet size and frequency are typically controlled by the modification of volumetric flow rates.<sup>3,4</sup> However, under constant flow rate conditions, only a few recent methods exist to dynamically control droplet properties, including mechanical actuation,<sup>5</sup> electro-wetting,<sup>6</sup> local heating,<sup>7</sup> and electric field application.<sup>8</sup>

In the past few years, the development of optofluidics has mainly focused on the use of microfluidic elements as new optical systems.<sup>9</sup> Conversely, light also represents a non-contacting external stimulus

that could control flows<sup>10</sup> and different fluidic operations (dividing, mixing, sorting).<sup>11</sup> However, only a few examples of light actuation applied to a two-phase flow in microchannels have been reported. Light has been used for macroscopic droplet manipulation<sup>12</sup> and perturbation of liquid interfaces through radiation pressure<sup>13</sup> or heating.<sup>14</sup> In microfluidic systems, it has only been used to generate droplets by laser-induced cavitation<sup>15</sup> and to modify the size<sup>16</sup> and the position<sup>17</sup> of droplets through a thermocapillary effect.

Here we describe the first approach to dynamically switch by light a two-phase flow from a laminar regime where the interface is not fragmented to a regime where droplets are formed. The introduction of a photosensitive surfactant<sup>12,18</sup> in the aqueous phase allows a photodependent modification of the wettability of the microchannel substrate. Under UV light, the interfacial energy of the aqueous phase on the substrate increases, which induces liquid fragmentation into monodisperse droplets. When the light stimulus stops, the system goes back to the laminar regime. Applicable to different device morphologies, this strategy allows many cycles of reversible and rapid switches as well as a spatio-temporal control of switch localization.

Fig. 1 shows our concept and experimental system. For all experiments, we used a cationic photosensitive azobenzene trimethylammonium bromide surfactant (AzoTAB)<sup>12,18</sup> in water (10 mM) as a photosensitive aqueous phase and oleic acid as oil phase. AzoTAB apolar tail contains a photosensitive azobenzene group, which photo-isomerizes from *trans* (less polar) to *cis* (more polar) configuration upon UV illumination (Fig. 1A). This concentration was chosen slightly below CMC (12.6 mM and 14.6 mM for *trans*- and *cis*- isomers, respectively).<sup>18</sup> Lower concentrations led to a decrease in stable laminar regimes. We did not explore higher concentrations due to the proximity of the solubility limit (~20 mM). We measured advancing and receding contact angles of AzoTAB solution in oleic acid on the substrate used for microfluidic experiments (plasma-treated and baked glass), and compared to those for the same AzoTAB solution having been illuminated under UV light prior to deposition. We found that the value increased from 153° and 148° (before UV) to 163° and 153° (after UV) for advancing and receding contact angles, respectively (Fig. 1B). We anticipated that this photo-induced change of wettability could have dramatic effects<sup>19</sup> when implemented in a microfluidic device for droplet generation (Fig. 1C). In particular, a two-phase microfluidic flow could be switched by light from a laminar regime under conditions of high wettability (–UV) to a droplet regime for lower wettability situation (+UV). Because of the continuous regeneration of the aqueous phase in the

<sup>a</sup>Department of Chemistry, Ecole Normale Supérieure, Paris, France. E-mail: damien.baigl@ens.fr; Fax: +33 1 4432 2402; Tel: +33 1 4432 2405

<sup>b</sup>Université Pierre et Marie Curie Paris 6, 4 place Jussieu, Paris, France

<sup>c</sup>UMR 8640, CNRS, France

<sup>d</sup>Center for Microfluidics and Nanotechnology, Peking University, Beijing, 100871, China

† Electronic supplementary information (ESI) available: Experimental section; Movies S1–S3 showing UV-induced reversible drop-drop, tube-drop, and tube-tube transitions; Movie S4 showing several cycles of tube-drop transition; Movie S5 showing the spatially-resolved light-induced droplet generation; movie legends; Fig. S1 and S2. See DOI: 10.1039/c1lc20328b

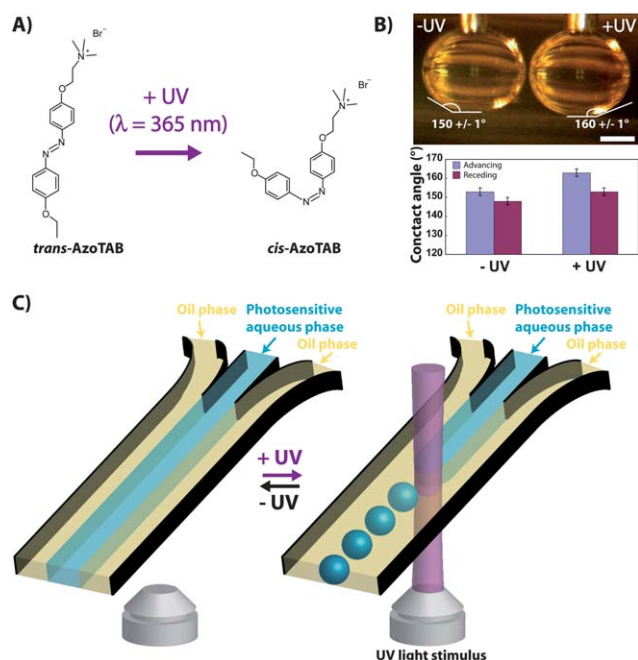


**Fig. 1** A photosensitive liquid in a two-phase microfluidic flow. (A) Molecular structure of the photosensitive surfactant AzoTAB. Upon illumination at  $\lambda = 365$  nm, *trans*-AzoTAB isomerizes to *cis* configuration, resulting in a more polar tail. (B) *Top*, contact angle measurement of a 10 mM AzoTAB aqueous solution droplet immersed in an oleic acid bath on the substrate used for microfluidic experiments (glass exposed to plasma and baked at 150 °C for 1 h). On the left, the AzoTAB solution contains a majority of *trans* molecules. On the right, the same solution has been exposed to UV light (majority of *cis* molecules) prior to droplet deposition. Scale bar is 1 mm. *Bottom*, values of advancing and receding contact angles before and after UV illumination, averaged on 10 replicates. (C) When this system is implemented in a two-phase microfluidic flow (10 mM AzoTAB solution as a photosensitive aqueous phase, oleic acid as an oil phase), the UV-induced change of substrate wettability can be used to control liquid fragmentation by light.

microchannel, turning off the light stimulus shall switch the system back to the laminar regime.

First we used Device 1, which has a standard flow focusing geometry with a neck (Fig. 2A). In the absence of UV illumination and for a given oil flow rate  $Q_{oil}$ , two regimes can be distinguished depending on the aqueous flow rate  $Q_{aq}$ .<sup>20</sup> At a low  $Q_{aq}$ , interfacial forces dominate and the aqueous phase is continuously fragmented into regular droplets ('drop' regime). At a high  $Q_{aq}$ , viscous forces are predominant and the aqueous phase is flowing parallel to the oil phase to form a stable tube ('tube' regime). Alternation of 'drop' and 'tube' regimes is eventually observed for a narrow range of intermediate  $Q_{aq}$ . In addition, for a given  $Q_{aq}$ , an increase in  $Q_{oil}$  has almost no influence on the regime nature but induces a decrease in the characteristic droplet or tube diameter. There is also a maximum oil flow rate  $Q_{oil}^{max}$ , above which the flow becomes mainly composed by the oil phase and stable water flow cannot be observed. The value of  $Q_{oil}^{max}$ , represented by a solid black line in Fig. 2B, increases with an increase in  $Q_{aq}$ . Below  $Q_{oil}^{max}$ , when UV illumination was applied on the flow regimes, three behaviours were observed depending on aqueous and oil flow rates (Fig. 2B). When the system is initially in a 'drop' regime ( $Q_{aq} < 2 \mu\text{L min}^{-1}$ ), UV illumination does not affect

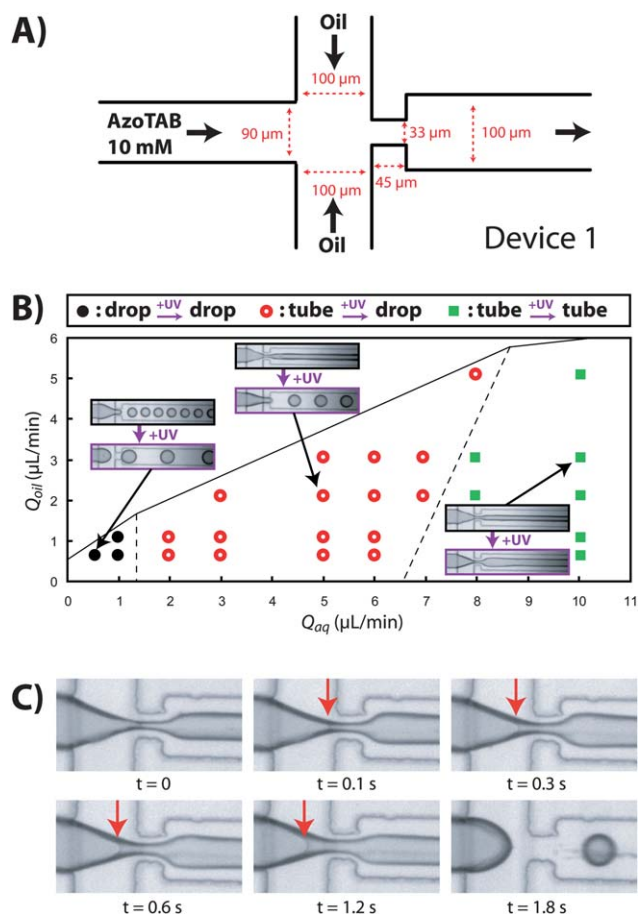


**Fig. 2** Effect of UV illumination on flow regimes. (A) Scheme of microfluidic Device 1. (B) Effect of UV illumination for different flow rates of oleic acid ( $Q_{oil}$ ) and AzoTAB solution ( $Q_{aq}$ ) in Device 1. The different symbols correspond to different transitions between a stable flow regime ('drop' or 'tube') without UV to another stable flow regime under UV illumination. Pictures correspond to the conditions of symbols pointed by arrows. The pictures of the regime under UV light have been taken 3 seconds after illumination starts. Above the solid line, the flow becomes monophasic (oil phase only). Dashed lines qualitatively indicate the separation between the different transitions induced by UV illumination. (C) Time-lapse observation of the UV-induced dewetting transition for the tube  $\rightarrow$  drop transition.  $t = 0$  corresponds to the beginning of UV illumination. The red arrow indicates the position of the contact line between the water phase and the microfluidic substrate.  $Q_{aq} = 3 \mu\text{L min}^{-1}$ ;  $Q_{oil} = 2 \mu\text{L min}^{-1}$ .

the regime nature but induces an increase in droplet diameter, which varies between 5% and 30% ('drop'  $\rightarrow$  'drop' transition, ESI†, Movie S1). When the system is initially in a 'tube' regime (middle and high aqueous flow rates), two effects can be distinguished. For  $2 \leq Q_{aq} \leq 7 \mu\text{L min}^{-1}$ , the 'tube' regime is converted to a stable 'drop' regime under UV illumination, regardless of  $Q_{oil}$  ('tube'  $\rightarrow$  'drop' transition, ESI†, Movie S2). For  $Q_{aq} \geq 8 \mu\text{L min}^{-1}$ , the system stays in a 'tube' regime for most  $Q_{oil}$  values ('tube'  $\rightarrow$  'tube' transition, ESI†, Movie S3) except for  $Q_{oil} = 5 \mu\text{L min}^{-1}$  where a transition to a 'drop' regime was observed.

All these results show that UV illumination results in a modification of the flow behaviour, which is particularly dramatic for intermediate aqueous flow rates ( $2 \leq Q_{aq} \leq 7 \mu\text{L min}^{-1}$ ) where a laminar liquid flow is fragmented into monodisperse droplets by light



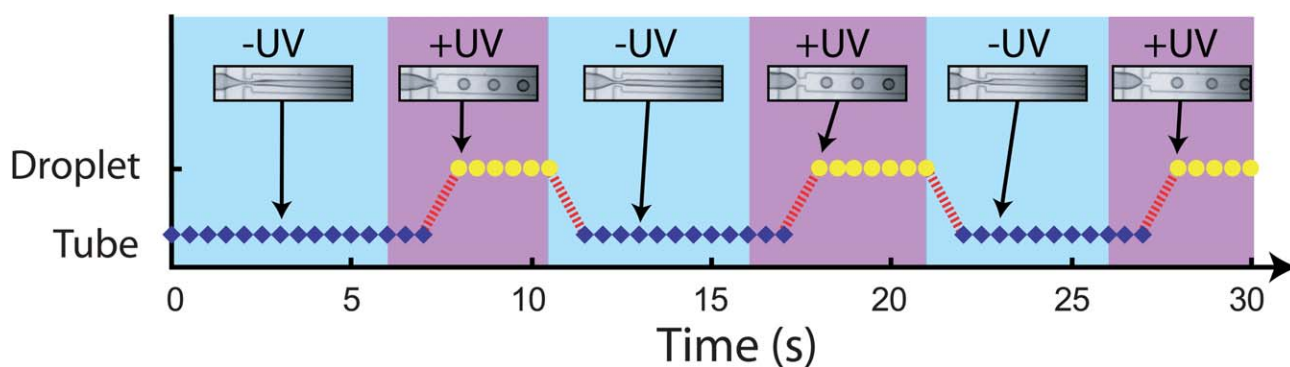


**Fig. 3** Fast and reversible liquid fragmentation by light. Continuous alternation of absence (–UV, light blue background) and presence (+UV, purple background) of UV illumination on a two-phase flow of AzoTAB solution ( $Q_{\text{aq}} = 3 \mu\text{L min}^{-1}$ ) and oleic acid ( $Q_{\text{oil}} = 2 \mu\text{L min}^{-1}$ ) in Device 1. Blue diamonds and yellow circles indicate stable ‘tube’ and ‘drop’ regimes, respectively. Red dashed lines indicate transient regimes. Pictures were extracted from Movie S4† and correspond to the conditions of symbols pointed by arrows.

(‘tube → drop’ transition). A usual and simple way to analyze biphasic microfluidic flow regimes consists in computing the capillary number  $Ca = \mu v / \gamma$  with  $\mu$  and  $v$  being the viscosity and the velocity of the continuous phase (here, oil) and  $\gamma$  the oil/water interfacial tension. By taking into account the geometry of our device,<sup>21</sup> we can estimate  $v$  to vary between  $1.9 \times 10^{-3}$  and  $19 \times 10^{-3} \text{ m s}^{-1}$  when  $Q_{\text{oil}}$  varies between 0.5 and  $5 \mu\text{L min}^{-1}$ . In the absence of UV,  $\gamma$  is around<sup>12</sup>  $7 \text{ mN m}^{-1}$  and  $Ca$  varies between  $0.75 \times 10^{-2}$  and  $7.5 \times 10^{-2}$ . Under UV,  $\gamma$  is around<sup>12</sup>  $8 \text{ mN m}^{-1}$  and  $Ca$  varies between  $0.65 \times 10^{-2}$  and  $6.5 \times 10^{-2}$ . These figures indicate that, regardless of conditions,  $Ca < 0.1$  showing that if we neglect the effect of substrate, capillary forces should maintain the system in a drop regime. The appearance of a stable tube regime demonstrates the crucial effect of the wetting of the AzoTAB solution on the microfluidic substrate. It is interesting to note that this is only observed for sufficiently high concentration of AzoTAB (here, 10 mM). For instance, with  $[\text{AzoTAB}] = 2 \text{ mM}$ , mainly drop regimes are observed, with and without UV illumination (ESI†, Fig. S1). We thus interpret the effect of UV light in the ‘tube → drop’ transition as a consequence of the light-induced change of wettability. Before illumination, *trans*-AzoTAB solution is wetting the substrate, which is confirmed by the angular shape of the meniscus, and forms a stable ‘tube’ regime. After illumination, AzoTAB isomerizes into the *cis* form. The resulting decrease in substrate wettability destabilizes the ‘tube’, induces its fragmentation into droplets and leads to a stable ‘drop’ regime, where the flow focusing part (round shape) does not wet the substrate anymore. This UV-induced dewetting transition of the water phase at the flow focusing region can be observed by following the contact line between the water phase and the substrate (Fig. 2C). To confirm this mechanism, we introduced *cis*-AzoTAB (low substrate wettability) in the microfluidic device (ESI†, Fig. S2). For  $Q_{\text{oil}} = Q_{\text{aq}} = 2 \mu\text{L min}^{-1}$ , we observed a stable drop regime in the absence of illumination. Under blue light, AzoTAB isomerized to the *trans* form, the substrate wettability increased and the system switched into a stable tube regime. When illumination was removed, the system switched back to the stable drop regime. All these results demonstrate the correlation between AzoTAB isomeric form (*trans* or *cis*), substrate wettability, and nature of the flow regime. This interpretation is in agreement with the classical observation that microfluidic channels with a low wettability favour emulsification and therefore formation of droplets.<sup>22</sup>

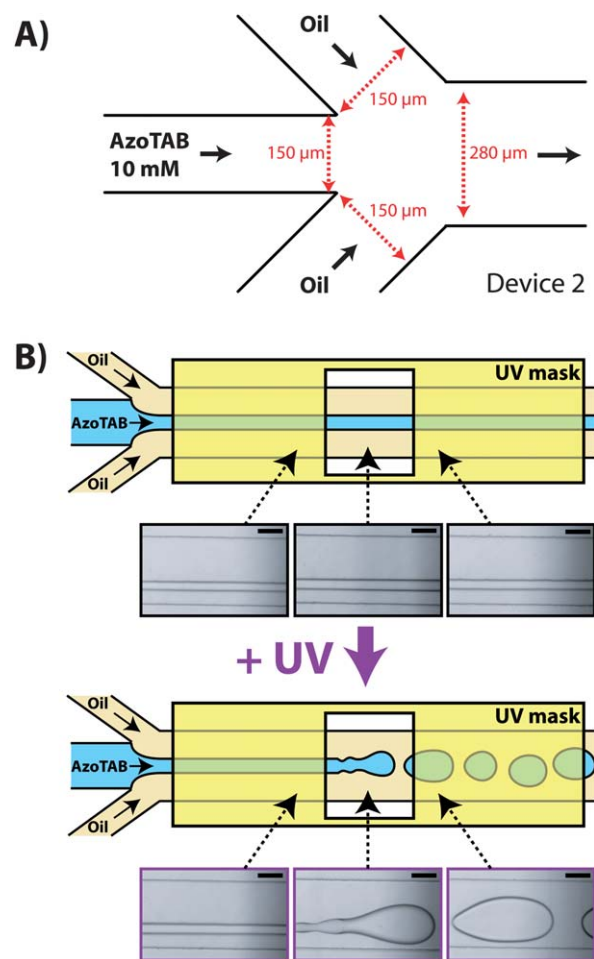


**Fig. 4** Spatially-selective fragmentation of a two-phase flow by light. (A) Scheme of microfluidic Device 2. (B) UV is applied on Device 2 through a transparent window made in a UV-cutting mask (yellow rectangle). Pictures show stable regimes just before, in the middle, and just after the window transparent to UV for a two-phase flow of AzoTAB solution ( $Q_{\text{aq}} = 1.5 \mu\text{L min}^{-1}$ ) and oleic acid ( $Q_{\text{oil}} = 2.4 \mu\text{L min}^{-1}$ ). All scale bars are  $100 \mu\text{m}$ .

For all UV-induced transitions shown in Fig. 2B, switching off UV results in a comeback to the initial flow regime (ESI†, Movies S1–S3), which can be explained by the continuous regeneration of the aqueous phase at the flow focusing junction. Interestingly, for  $2 \leq Q_{\text{aq}} \leq 7 \mu\text{L min}^{-1}$ , several cycles of ‘tube  $\rightarrow$  drop  $\rightarrow$  tube’ can be obtained by successively switching on and off UV illumination (Fig. 3, ESI†, Movie S4). Regardless of flow rate conditions and transition type, the switching occurs within 2 s. All these results demonstrate that our method allows one to fragment by light a liquid in a reversible and highly dynamic manner.

In Device 1, when liquid fragmentation occurs, droplets are generated in the neck area where the two liquid phases are strongly confined. To spatially control the localization of droplet generation using light, we applied selective UV illumination through a photo-mask on Device 2, which is a flow focusing device without any constriction (Fig. 4A). In the absence of UV illumination, the system is in a stable ‘tube’ regime all along the main channel for a large range of flow rates ( $1 \leq Q_{\text{aq}} \leq 15 \mu\text{L min}^{-1}$ ;  $2 \leq Q_{\text{oil}} \leq 13 \mu\text{L min}^{-1}$ ). When UV is applied, only the channel part above the mask window is illuminated and we observe within a few seconds (i) a stable ‘tube’ regime just before the mask window, (ii) a droplet generation part in the middle of the illuminated area, and (iii) a stable regime of slightly irregular droplets right after the mask window (Fig. 4B, ESI†, Movie S5). This effect was reproducibly observed for arbitrary positions of the mask window and intermediate aqueous flow rates ( $1.5 \leq Q_{\text{aq}} \leq 5 \mu\text{L min}^{-1}$ ;  $2.4 \leq Q_{\text{oil}} \leq 13 \mu\text{L min}^{-1}$ ). When UV is switched off, the system goes back to a stable ‘tube’ regime all along the main channel. This constitutes the first demonstration that an external stimulus (here, light) can reversibly control the localization of the fragmentation of a liquid into microdroplets.

In summary, we have reported for the first time the fragmentation of a continuous aqueous liquid phase into monodisperse microdroplets by light actuation. The liquid response to the light stimulus has been demonstrated to be robust, fast, reversible, and spatially resolved. Our method, which only implies the addition of a photosensitive surfactant in the aqueous phase, can be easily implemented into various microfluidic and optofluidic configurations, opening the route to the generation of all-optical fluidic chips, where fluids are both sample and optical elements and light serves as both actuator and sensor. In future, this method of light-induced liquid segmentation could also be applied for high-throughput compartmentalization and encapsulation of shear-sensitive biological material, such as living cells or genomic DNA molecules.

## Acknowledgements

We thank M. Abkarian for a decisive discussion. The research leading to these results has received funding from the European Research Council under the European Community's Seventh Framework Programme (FP7/2007-2013)/ERC Grant agreement no. 258782.

## Notes and references

- (a) G. M. Whitesides, *Nature*, 2006, **442**, 368–373; (b) H. Song, D. L. Chen and R. F. Ismagilov, *Angew. Chem., Int. Ed.*, 2006, **45**, 7336–7356; (c) A. J. de Mello, *Nature*, 2006, **442**, 394–402.
- (a) M. Joanicot and A. Ajdari, *Science*, 2005, **309**, 887–888; (b) J. Atencia and D. J. Beebe, *Nature*, 2005, **437**, 648–655; (c) T. M. Squires and S. R. Quake, *Rev. Mod. Phys.*, 2005, **77**, 977–1026.
- (a) T. Thorsen, R. W. Roberts, F. H. Arnold and S. R. Quake, *Phys. Rev. Lett.*, 2001, **86**, 4163–4166; (b) S. L. Anna, N. Bontoux and H. A. Stone, *Appl. Phys. Lett.*, 2003, **82**, 364–366.
- (a) P. Garstecki, M. J. Fuerstman, H. A. Stone and G. M. Whitesides, *Lab Chip*, 2006, **6**, 437–446; (b) V. van Steijn, C. R. Kleijn and M. T. Kreutz, *Lab Chip*, 2010, **10**, 2513–2518.
- (a) A. R. Abate, M. B. Romanowsky, J. J. Agresti and D. A. Weitz, *Appl. Phys. Lett.*, 2009, **94**, 023503; (b) A. Bransky, N. Korin, M. Khoury and S. Levenberg, *Lab Chip*, 2009, **9**, 516–520.
- H. Gu, F. Malloggi, S. A. Vanapalli and F. Mugele, *Appl. Phys. Lett.*, 2008, **93**, 183507.
- N.-T. Nguyen, T.-H. Ting, Y.-F. Yap, T.-N. Wong, J. C.-K. Chai, W.-L. Ong, J. Zhou, S.-H. Tan and L. Yobas, *Appl. Phys. Lett.*, 2007, **91**, 084102.
- D. R. Link, E. Grasland-Mongrain, A. Duri, F. Sarrazin, Z. Cheng, G. Cristobal, M. Marquez and D. A. Weitz, *Angew. Chem., Int. Ed.*, 2006, **45**, 2556–2560.
- D. Psaltis, S. R. Quake and C. H. Yang, *Nature*, 2006, **442**, 381–386.
- A. Terray, J. Oakey and D. W. M. Marr, *Science*, 2002, **296**, 1841–1844.
- (a) J. Glückstad, *Nat. Mater.*, 2004, **3**, 9–10; (b) S. L. Neale, M. P. Macdonald, K. Dholakia and T. F. Krauss, *Nat. Mater.*, 2005, **4**, 530–533; (c) G. L. Liu, J. Kim, Y. Lu and L. P. Lee, *Nat. Mater.*, 2006, **5**, 27–32.
- A. Diguët, R.-M. Guillemic, N. Magome, A. Saint-Jalmes, Y. Chen, K. Yoshikawa and D. Baigl, *Angew. Chem., Int. Ed.*, 2009, **48**, 9281–9284.
- A. Ashkin and J. M. Dziedzic, *Phys. Rev. Lett.*, 1973, **30**, 139–142.
- N. Garnier, R. O. Grigoriev and M. F. Schatz, *Phys. Rev. Lett.*, 2003, **91**, 054501.
- S.-Y. Park, T.-H. Wu, Y. Chen, M. A. Teitell and P.-Y. Chiou, *Lab Chip*, 2011, **11**, 1010–1012.
- C. N. Baroud, J.-P. Delville, F. Gallaire and R. Wunenburger, *Phys. Rev. E: Stat., Nonlinear, Soft Matter Phys.*, 2007, **75**, 046302.
- (a) K. T. Kotz, K. A. Noble and G. W. Faris, *Appl. Phys. Lett.*, 2004, **85**, 2658–2660; (b) J.-P. Delville, M. Robert de Saint Vincent, R. D. Schroll, H. Chraïbi, B. Issenmann, R. Wunenburger, D. Lasseux, W. W. Zhang and E. Brasselet, *J. Opt. A: Pure Appl. Opt.*, 2009, **11**, 034015.
- (a) A. Estévez-Torres, C. Crozatier, A. Diguët, T. Hara, H. Saito, K. Yoshikawa and D. Baigl, *Proc. Natl. Acad. Sci. U. S. A.*, 2009, **106**, 12219–12223; (b) A. Diguët, N. K. Mani, M. Geoffroy, M. Sollogoub and D. Baigl, *Chem.–Eur. J.*, 2010, **16**, 11890–11896.
- R. Dreyfus, P. Tabeling and H. Willaime, *Phys. Rev. Lett.*, 2003, **90**, 144505.
- P. Guillot and A. Colin, *Phys. Rev. E: Stat., Nonlinear, Soft Matter Phys.*, 2005, **72**, 066301.
- S. L. Anna and H. C. Mayer, *Phys. Fluids*, 2006, **18**, 121512.
- (a) T. Kawakatsu, G. Tragardh, C. Tragardh, M. Nakajima, N. Oda and T. Yonemoto, *Colloids Surf., A*, 2001, **179**, 29–37; (b) W. Li, Z. Nie, H. Zhang, C. Paquet, M. Seo, P. Garstecki and E. Kumacheva, *Langmuir*, 2007, **23**, 8010–8014; (c) L. M. Fidalgo, C. Abell and W. T. S. Huck, *Lab Chip*, 2007, **7**, 984–986.